A Study on Low Cycle Fatigue Life Assessment of Notched Specimens Made of 316LN Austenitic Stainless Steel

Ikram Abarkan
SCD Laboratory, Department of Physics, Faculty of Sciences, Abdelmalek Essaadi University, Tetouan, Morocco
aberkan.ikraam@gmail.com

Abdellatif Khamlichi
SCD Laboratory, ENSA Tetouan, Abdelmalek Essaadi University, Tetouan, Morocco
khamlichi7@yahoo.es

Rabee Shamass
Division of Civil and Building Services Engineering, School of the Built Environment and Architecture, London South Bank University, UK
shamassr@lsbu.ac.uk

ABSTRACT

The local strains obtained from the best-known analytical approximations namely; Neuber's rule, Equivalent Strain Energy Density method, and linear rule, were compared with those resulting from finite element analysis. It was found that apart from Neuber's rule with the elastic stress concentration factor K_t, all the aforementioned analytical methods underestimate the local strains for all notch root radius, strain amplitudes levels, at room temperature and 550 °C. Neuber's rule with K_t slightly overestimates the maximum strains for lower notch root radius, namely 1.25 mm, at high temperature. Based on the analytically and numerically obtained notch root strains, the fatigue lives were estimated using the Coffin-Manson-Basquin equation. Besides, a numerical assessment of fatigue lives was made based on Brown-Miller and maximum shear strain multiaxial fatigue life criteria. It was found that all these methods provide inaccurate fatigue life results for all notch root radius, strain amplitude level, and under both temperatures conditions. Therefore, a new method was suggested, for which only the applied strain amplitude is needed to calculate the fatigue life of notched components. It was revealed that the suggested-method provides a good fatigue life prediction at a higher temperature loading state.

Keywords: Finite element analysis, 316 LN stainless steel, notched specimens, local strain approaches, low cycle fatigue.

1 Introduction

Engineering components such as shafts in vehicles, pistons in engines, and many other mechanical parts are frequently subjected to cyclic loadings during their service, which makes fatigue failures more common. Like any other type of failure, failure due to fatigue occurs in the stress concentration regions as a result of discontinuities in the structures such as holes, grooves, fillets, and welds, which are generally known as notches. The presence of the notches in a part generates a multiaxial state of stress in the material and makes the fatigue life predictions more complicated.

The estimation of the fatigue life of notched components completely relies on a reliable determination of the stresses and strains components at the notch-root. The assessment of the material response at the notch-tips could be made experimentally, numerically, or based on analytical rules. Since the experimental determination of the local stress and strain is expensive and laborious, numerical and analytical evaluations are more often used in the field of engineering. The most commonly applied numerical tool for predicting the stresses and strains for elastic-plastic behavior at the notch-tips is the Finite Element Analysis (FEA). This method has proven to be efficient, reliable and sufficiently precise. Another kind of non-linear stress-strain assessment consists of applying analytical approximations such as Neuber's rule [1], and Equivalent Strain Energy Density (ESED) method [2,3]. Over time, extensive research has been conducted to evaluate the accuracy of the Neuber's rule [1] and the ESED method [2,3] to predict the strains in notched components. In general, it has been found that in the event of elastic-plastic problems, the Neuber's rule [1] overestimates the strains at the notch-tip, whereas the ESED

relation [2,3] underestimates the local strains [4]. Substantial efforts have been made to improve the accuracy of Neuber and ESED relations [1-3] for several materials, notch geometries, and types of load. Particularly, Topper et al. [5] extended the Neuber's rule to fatigue studies by replacing the elastic stress concentration factor K_t with the fatigue stress concentration factor K_f. Hoffmann and Seeger [6] suggested a generalization of the Neuber's rule [1] to multiaxial elastic-plastic notch problems under monotonic and cyclic loading. To account for the general yielding in the net section, Seeger and Heuler [7] introduced a generalized formula of Neuber's rule that accounts for various notch geometries and loadings. To consider the effect of the notch root constraint, Fuchs and Stephens [8] proposed a modification of the cyclic Neuber's rule [1] by introducing an exponent noted m on the ratio $\Delta\sigma/\Delta S K_t$, where $\Delta\sigma$ and ΔS are the local and nominal stress range, respectively. Wang and Sharpe [9] re-examined the modified Neuber's rule suggested by Fuchs and Stephens [8] for aluminum specimens and found out that the modified-version gives a better prediction of axial strains compared to the local strains predicted by the original Neuber's rule [1]. Based on the concept of the total strain energy density proposed by Neuber [1] and the Equivalent Strain Energy Density envisaged by Molski and Glinka [2] and Glinka [3], Moftakhar et al. [10] presented a method allowing the evaluation of the non-linear stress-strain behavior at the notch tips in the case of multi-axial cyclic loading problems. Singh et al. [11] suggested a method which enables the determination of the elastic-plastic strain at the notch tips for structures under uniaxial or multiaxial nominal cyclic loads. More recently, Ye et al. [12] demonstrated that the Neuber's rule [1] is a particular case of the ESED method [2,3]; that is to say when the plastic strain energy is ignored in the ESED method [2,3], both Neuber's rule [1], and the ESED method [2,3] become identical. Meanwhile, they developed a modified version of

the ESED method [2,3] that considers the heat energy dissipated during one loading cycle instead of the plastic strain energy in the local strain approach. Campagnolo et al. [13] carried out a detailed theoretical and numerical study on the elastic-plastic behavior of three-dimensional notched components under multiaxial cyclic loading, it was found that the obtained local strains from FEA and that resulted from Ye et al. [12] suggested method are well correlated. A modified version of the ESED method [2,3] was also introduced by Li et al. [14], where a factor of $(1+\nu_e)/(1+\nu_{eff})$ was incorporated to modify the heat energy included in the ESED equation [2,3], where ν_e and ν_{eff} are the elastic and the effective Poisson's ratio respectively. This method was proven to be valid for monotonic, and uniaxial Low Cycle Fatigue (LCF) loads. Zhu et al. [15] proposed a modification in the ESED method [2,3] by including the effective Poisson's ratio ν_{eff} to correct the dissipated heat energy in the original ESED equation [2,3].

In addition to the Neuber's rule [1], and the ESED method [2,3], Barkey et al. [16] developed an analytical approach to determine the non-linear local strains for isotropic notched materials undergoing a multiaxial cyclic loading state, relying on the notion of the structural yield surface. This method counts on the anisotropic plasticity theory to establish the structural yield surface in nominal stress space that combines the isotropic material properties and the anisotropic geometry factors of notch [16]. Based on the same concept, Köttgen et al. [17] suggested two related approaches namely, the pseudo-stress and the pseudo-strain approaches, which can be applied for low cycle fatigue uniaxial and multiaxial nominal loads problems. Over time, many research studies have been conducted to correct the inaccuracy of Köttgen et al. [17], in particular, Hertel et al. [18] modified the Köttgen et al. [17] method by applying Jiang's plasticity model [19] to improve the stress-strain assessment for low cycle fatigue multiaxial loading. Most

recently, Firat [20] introduced a new model based upon the Chaboche cyclic plasticity relation [21] to determine the multiaxial strains of notched specimens under tensile and torsion loadings for 1070 steel. In reliance on the multiaxial Radial Return Method, Antoni [22] suggested a new method to assess the multiaxial elastic-plastic behavior at the notch. This method can be applied to analytical elastic problems and complex three-dimensional elastic-FE analyses.

The 316 LN Stainless Steel (SS) is one of the most widely used materials in engineering practice, especially in liquid metal cooled fast breeder reactors, owing to high corrosion resistance and excellent mechanical properties [23]. Over the years, extensive research studies have been made to examine the low cycle fatigue of smooth specimens made of 316 LN SS in different environments and at various temperature loading conditions [24-28]. More recently, Abarkan et al. [29] studied the low cycle fatigue behavior of smooth cylindrical specimens made of this material at room temperature conditions, by mean of different numerical and analytical methods. Due to inaccuracy of predicted lives obtained from some analytical models, they proposed new parameters to correct the disparities between the analytical results and the experimental data. Nevertheless, little research exists in the literature on the low cycle fatigue behavior of notched samples made of 316LN SS [30,31]. Therefore, it is important to investigate the ability of notched specimens made of 316 LN stainless steel in withstanding uniaxial cyclic loadings, when both the net section and the notch root are under a plastic loading state, in both room and higher temperatures.

The conventional way for evaluating the fatigue life of components with notches consists of first determining numerically or analytically the local stress-strain at the notch root, then calculating the fatigue life using the commonly known strain-life equation with the fatigue data associated

to smooth samples. However, this method is lengthy and tedious. Moreover, any inaccurate prediction of local strain at the notch root will lead to erroneous fatigue life. The present work aims to establish a new method that allows the estimation of low cycle fatigue life using the nominal strain as an input parameter instead of using local strain to predict fatigue life using the Coffin-Manson-Basquin equation [32-34]. This method has been examined for samples made of 316LN stainless steel at room temperature and 550 °C with different U-notch root sizes. It has been revealed that the obtained LCF life results correlate well with the experimental ones obtained by Agrawal et al. [31] at a high-temperature state. A comparison of the local strains obtained from analytical methods namely, the Neuber's rule [1,5], the ESED method [2,3] and the linear rule [35] with those obtained from FEA was made, and the cyclic life was determined using the Coffin-Manson-Basquin equation [32-34]. Based on the numerical evaluation of the local strains, an attempt was made to predict the fatigue life using multiaxial strain-life equations specifically, Brown-Miller [36] and maximum shear strain life [37] criteria both with Morrow mean stress correction [38].

2 Experimental Details

Agrawal et al. [31] carried out a uniaxial fully reversed ($R_\varepsilon = -1$) low cycle fatigue experiment on twenty-four specimens, at room temperature and 550 °C. The test was conducted on six plain specimens; three were tested at room temperature, and the other three were tested at 550 °C. The remaining eighteen specimens were circumferentially notched ones, with a different notch root radius of 1.25, 2.5, and 5 mm, and a constant notch root depth of 1.465 mm. Nine of them were tested at room temperature, and the other nine were tested at 550 ° C. The plain, and the notched specimens with a gauge length of 28 and 10 mm gauge diameter were loaded at a

constant strain rate of 3×10^{-3} s^{-1}, at various strain amplitudes namely, ± 0.4, ± 0.6, and ± 0.8%. *Figure 1* and *Figure 2* depict the geometry and the dimensions of plain and notched specimens, respectively.

3 Finite Element Analysis

Smooth and notched specimens subjected to fully reversed uniaxial cyclic loading were modeled using finite element analysis on ABAQUS/Standard software [39]. The 2D-axisymmetric model that represents the gauge section of the smooth and notched specimens, has a 5 mm radius and a 12.5 mm in height, was meshed using the CAX4R elements, which are 4-node bilinear elements with reduced integration and hourglass control, generally used in axisymmetric finite element stress studies, and for simulation involving large-strain analysis. Mesh refinement technique was employed near the notch roots as seen in *Figure 3(a)* to ensure accurate prediction of elastic stress concentration factor as well as the local stresses and strains. Symmetry boundary conditions were applied along the gauge length and the gauge diameter. The prescribed displacement model was implemented on the top edge of the FE model, as illustrated in *Figure 3(b)*, and the predefined temperature was applied and fixed at 550 °C for isothermal low cycle fatigue analysis. The material properties implemented in the ABAQUS [39] are represented in *Table 1* for both temperatures.

4 Results and Discussion

4.1 Cyclic Stress-Strain Behavior

Since the experimental hysteresis loops are not provided by Agrawal et al. [31], a FE simulation with the same characteristics mentioned in *section 3* was performed on a modified 9Cr-1Mo steel

[40], and the numerical model was validated, by comparing the numerical hysteresis loops with the experimental ones given by Veerababu et al. [40]. *Figure 4* shows a comparison between the numerical and the experimental stress-strain curve for a plain specimen with the same geometry and dimensions represented in *Figure 1,* and subjected to ± 0.3, and ± 0.8 % strain amplitudes, at 550 °C. As it can be observed, the numerically obtained hysteresis loops match well with experimental ones, which indicates that the FE model is totally correct. It should be pointed out that the FE model was simulated using Chaboche material parameters [41] provided by Veerababu et al [40]. More details about the material model implementation are mentioned in Abarkan et al. paper [29]. *Figure 5* depicts the local stress-strain behavior (i.e. at the notch-tip) obtained from the current FEA simulation and the one carried out by Veerababu et al. [40] for a specimen with the same shape and dimensions shown in *Figure 2-(a)* under ±149.95MPa nominal stress amplitude and at 550°C temperature level. As it can be noticed, the numerically obtained local stress-strain curves using FE analysis are in good agreement with the one found numerically by Veerababu et al. [40]. As Chaboche parameters are not provided by Agrawal et al. [31] for 316LN SS, Ramberg-Osgood material model [42] was implemented in FE simulations to determine the maximums strains and subsequently the cyclic life.

It should be pointed out that the analysis of the cyclic stress behavior (i.e. maximum stress vs the number of cycles) of smooth samples under different imposed strain amplitudes, at room temperature and 550 °C, revealed that the present study used material shows initial cyclic hardening succeeded by cyclic softening, and then saturation before final failure occurs. The initial cyclic hardening was observed to be significant for higher number of cycles at 550 °C than at room

temperature. Besides, at both temperatures, it was found that the range of initial hardening exhibited by this material decreases with the decrease of strain amplitude [31].

4.2 Notch-Root Strains Assessment

The local strains were determined using four different analytical approximations, namely, Neuber's rule with elastic stress concentration factor K_t[1], Neuber's rule with fatigue stress concentration factor K_f[5], ESED or Glinka's method [2,3] and the linear rule [35], as well as using the FEA.

Neuber's rule with K_t [1] relates the local stress range $\Delta\sigma$ and the local strain range $\Delta\varepsilon$ with the nominal stress and strain ranges ΔS and Δe, respectively, as follows:

$$\Delta\sigma\Delta\varepsilon = K_t^2\Delta S\Delta e \tag{1}$$

This equation can be solved for local strains by using the following Ramberg-Osgood equation [42].

$$\Delta\varepsilon = \frac{\Delta\sigma}{E} + 2\left(\frac{\Delta\sigma}{2K'}\right)^{\frac{1}{n'}} \tag{2}$$

where K' and n' are, respectively, the cyclic strength coefficient and the cyclic strain hardening exponent, and E is Young's modulus of the material. By substituting (2) in (1), one can obtain the following equation:

$$\frac{\Delta\sigma^2}{E} + 2\Delta\sigma\left(\frac{\Delta\sigma}{2K'}\right)^{\frac{1}{n'}} = K_t^2\Delta S\Delta e \tag{3}$$

In the case of a plastic net section (i.e. the applied stress is more than the yield stress of the SS), the nominal strain range Δe is related to the nominal stress range ΔS, by Ramberg-Osgood equation [42] as follows:

$$\Delta e = \frac{\Delta S}{E} + 2\left(\frac{\Delta S}{2K'}\right)^{\frac{1}{n'}} \tag{4}$$

Thus Eq. (1) and (3) take the following form respectively.

$$\Delta\sigma\Delta\varepsilon = K_t^2\frac{\Delta S^2}{E} + 2K_t^2\Delta S\left(\frac{\Delta S}{2K'}\right)^{\frac{1}{n'}} \tag{5}$$

$$\frac{\Delta\sigma^2}{E} + 2\Delta\sigma\left(\frac{\Delta\sigma}{2K'}\right)^{\frac{1}{n'}} = K_t^2\frac{\Delta S^2}{E} + 2K_t^2\Delta S\left(\frac{\Delta S}{2K'}\right)^{\frac{1}{n'}} \tag{6}$$

For a given nominal stress range ΔS, the local stress range $\Delta\sigma$ can be obtained from Eq.(6), and then the local strain range $\Delta\varepsilon$ from Eq.(5).

Neuber's rule with K_f proposed by Topper et al. [5] consists of replacing the elastic stress concentration factor K_t with the fatigue stress concentration factor K_f. The expression of K_f, which was suggested by Peterson [43], is as follows:

$$K_f = 1 + (K_t - 1)q \tag{7}$$

where q is the notch sensitivity factor, and it is expressed as follows [43]:

$$q = \frac{1}{1 + \rho/r} \tag{8}$$

r is the notch root radius, and ρ depends on material properties [43]:

$$\rho = 0.0254\left(\frac{2070}{S_u}\right)^{1.8} \tag{9}$$

where S_u is the ultimate tensile strength in *MPa*, and it is equal to 646 and 504 *MPa*, at ambient temperature and 550°C, respectively [31].

The values of the fatigue stress concentration factor K_f obtained from Eq.(7) are listed in the Table 2 for notch root radius of 1.25, 2.5, and 5 mm. The values of the elastic stress concentration factor K_t, which is defined as $K_t = \sigma/S = \varepsilon/e$ (σ,ε, S, and e are the local stress, the local strain, the nominal stress, and the nominal strain, respectively) have been found by performing an elastic FEA using ABAQUS software, and are summarized in the same table (i.e. Table 2).

On the other hand, the elastic strain energy density equation for fatigue problems proposed by Molski, and Glinka [2], and Glinka [3] is defined by as:

$$\frac{\Delta\sigma^2}{E} + \frac{4\Delta\sigma}{n'+1}\left(\frac{\Delta\sigma}{2K'}\right)^{\frac{1}{n'}} = K_t^2 \Delta S \Delta e \tag{10}$$

For a plastic net section, Eq. (10) becomes as:

$$\frac{\Delta\sigma^2}{E} + \frac{4\Delta\sigma}{n'+1}\left(\frac{\Delta\sigma}{2K'}\right)^{\frac{1}{n'}} = K_t^2 \frac{\Delta S^2}{E} + 2K_t^2 \Delta S \left(\frac{\Delta S}{2K'}\right)^{\frac{1}{n'}} \tag{11}$$

Thus, for a given nominal stress range ΔS, one can calculate the local stress range $\Delta\sigma$ from (Eq. (11), and the local strain range can eventually be found using Ramberg-Osgood equation (Eq. (2)) [42].

The linear rule [35] assumes that the elastic stress concentration factor K_t is the ratio of the local strain range $\Delta\varepsilon$ and to the nominal strain range Δe:

$$\Delta\varepsilon = K_t \Delta e \tag{12}$$

For a given Δe and K_t, one can easily obtain the local strain range $\Delta\varepsilon$ using Eq. (12).

The local strains obtained from the analytical approximations have been compared with those found from FE simulations. *Figure 6* and *Figure 7* illustrate the local strains of specimens with

notch root radius of 1.25, 2.5, and 5 mm under ± 0.4, ± 0.6, and ± 0.8% strain amplitudes, at room temperature and 550°C respectively. At room temperature conditions, it can be observed that Neuber's rule with K_t[1] underestimates the local strains for all notch root radius sizes and strain amplitudes. However, at higher temperature condition, it somewhat overestimates the local strains for lower notch radius sizes and underestimates the strains at higher notch radii. At normal and high temperature conditions, Neuber's rule with K_f[5], and ESED method [2,3] underestimate the maximum strains for all notch root radius sizes and strain amplitudes. However, the resulted relative error using the Neuber's rule with K_f[5] is less significant than those obtained using the ESED method [2,3] for all notch root sizes. For example, at room temperature, when the applied nominal strain is ± 0.6%, and the notch root radii is 2.5 mm, the obtained relative error using the Neuber's rule with K_f [5] and the ESED method [2,3] is -30.93 and -45.59% respectively. As it was expected, Neuber's rule with K_t [1] always predicts higher local strains than the ESED method [2,3], differently stated, the local strain results obtained from Neuber's rule [1] show close agreement with those found from FE analysis, while the local strain results resulted from the ESED method always lie below those provided from Neuber's rule, this is due to the presence of an extra-factor $2/(1+n')$ in the Eq. (11) for ESED method [2,3] as compared with Neuber's rule with K_t [1] presented by Eq.(6). Since the value of n' is always less than 1, the local strains calculated by the ESED method [2,3] are subsequently lower than those obtained by Neuber's rule with K_t [1]. From another aspect, Ye et al. [12] explained the disparities between these two methods [1-3] due to the fact that in the Neuber's relation [1], the dissipation of the plastic strain energy at the notch root is neglected i.e. it always equals to zero, and larger than zero in the case of ESED relation [2,3], as a result, Neuber's rule [1] will always lead to higher local strains

compared to the ones resulted from the ESED method [2,3]. The linear rule [35] also underestimates the local strain for all applied loads at both temperatures and all notch root radius. The relative error increases slightly as the strain amplitude increases. For instance, for a notch root radii of 2.5 mm, the relative error increases from -57.3 to -59.1 % and -37.3 to -42.1 % at room temperature and 550 °C, respectively. As it can be seen from *Table 3*, the relative error is higher at room temperature than at high-temperature, and for large notch root radius than for small notch radius.

4.3 Fatigue Life Estimation

In this section, fatigue lives will be evaluated using uniaxial low cycle fatigue method, specifically the Coffin-Manson-Basquin equation [32-34], and using multiaxial low cycle fatigue criteria, in particular, Brown-Miller [36] and maximum shear strain life equations [37] along with Morrow mean stress correction technique.

4.3.1 Fatigue Life Estimation Based on Uniaxial Low Cycle Fatigue Method

Long ago, Basquin [33] suggested the following stress-life relationship:

$$\frac{\Delta\varepsilon_e}{2} = \frac{\sigma_f'}{E}(2N_f)^b \tag{13}$$

On the other side Coffin [31] and Manson [32] separately introduced the following strain-life equation:

$$\frac{\Delta\varepsilon_p}{2} = \varepsilon_f'(2N_f)^c \tag{14}$$

where $\Delta\varepsilon_e$ and $\Delta\varepsilon_p$ are respectively the elastic and plastic strain ranges, σ_f' is the fatigue strength coefficient, ε_f' is the fatigue ductility coefficient, b is the fatigue strength exponent, c is the fatigue ductility exponent and N_f is the fatigue life.

Thus, the total strain range $\Delta\varepsilon_t$ can be related to the fatigue life N_f by the Coffin-Manson-Basquin equation [32-34] as follows:

$$\frac{\Delta\varepsilon_t}{2} = \frac{\Delta\varepsilon_e}{2} + \frac{\Delta\varepsilon_p}{2} = \frac{\sigma_f'}{E}(2N_f)^b + \varepsilon_f'(2N_f)^c \quad (15)$$

The experimental and predicted fatigue lives based upon the calculated total local strains obtained from Neuber's rule with K_t[1], Neuber's rule with K_f[5], ESED method [2,3], linear rule [35], and FEA are plotted in log-log scale, as depicted in *Figure 8* and *Figure 9* for room temperature and 550 °C respectively. In comparison with the experimental fatigue lives, it should be pointed out that the fatigue lives estimated at room temperature generally have less relative error compared to the fatigue lives obtained at the high temperature condition. In addition, the predicted fatigue lives using the local strains from Neuber's rule with K_t [1] are very conservative, especially at higher temperature level, where the relative error is –94.5% for 2.5 mm notch root radii and ± 0.6% strain amplitude. On the other hand the relative error is only –49.1% at room temperature for the same notch root radius and strain amplitude level. The expected fatigue lives based on the local strains calculated from Neuber's rule with K_f[5] have also led to much-underestimated results, mainly at 550°C. The relative errors for a notch root radius of 2.5 mm, and ± 0.6% strain amplitude at room temperature and 550 °C are –40.2 and -90.8%, respectively. However, the relative errors between the calculated fatigue lives from Neuber's rule with K_t [1], and the experimental ones are more relevant than the relative errors between the estimated

fatigue lives from Neuber's rule with K_f [5] and the experimental life data. On the other hand, the fatigue lives obtained from the ESED method [2,3] are conservative at high temperature for all notch root sizes, and room temperature for 1.25 mm notch size. Nonetheless, ESED method has generally resulted in non-conservative estimation for 2.5 and 5 mm notch root radii under room temperature condition, for some strain amplitude levels. By way of example, the relative errors at ± 0.8% strain amplitude are 10.2 and 12.1 % for 2.5 and 5 mm, respectively. Despite that the obtained fatigue lives using the linear rule [35] are conservative at 550 °C, with a maximum relative error of -80.9% for 5 mm notch root radius, under ± 0.8% strain amplitude condition, the resulting fatigue lives using this rule are non-conservative at room temperature with a maximum relative error of 96.88 % . The fatigue lives estimated from the numerically obtained local strains (FEA) are very conservative for room and elevated temperature, with a maximum relative error of -82.07 and –96.43 % at room temperature and 550°C, respectively. In *Table 4* are illustrated the values of the relative error between the predicted fatigue lives using the local strain approximation methods and the experimental ones as a function of temperature, applied strain amplitude and notch root radius. Overall, the calculated fatigue lives based on the local strains from the linear rule [35] are the closest to the experiment at high-temperature, and the fatigue lives found using the maximum strains from the ESED method [2,3] are the most realistic at room temperature loadings.

4.3.2 Fatigue Life estimation Based on Multiaxial Low Cycle Fatigue Methods

Since the presence of discontinuities in a component develops a multiaxial state of stress near the notch root, attempts have been undertaken to assess the fatigue life using multiaxial low cycle fatigue life methods, such as Brown-Miller and maximum shear strain life criteria. In the first

place, the cyclic stress-strain data for each notch root radius, strain amplitude level, and temperature conditions were imported from ABAQUS [39] into Fe-Safe fatigue software [44]. As the fatigue cracks usually initiate on the surface [45], the nodal values of the FE-model were selected, and the elastic-plastic block was created to take into consideration the elastic-plastic behavior of the material. The static and the cyclic properties of 316 LN SS listed in *Table 1* were implemented in the material databases in Fe-safe. The Brown-Miller [36] and maximum shear strain life [37] criteria along with the Morrow mean stress effect [38], i.e. Eq.(16) and Eq.(17) respectively were independently opted as algorithms in Fe-Safe for fatigue analysis.

$$\left(\frac{\Delta\gamma}{2}+\frac{\Delta\varepsilon_n}{2}\right)_{max}=1.65\frac{\sigma_f'-\sigma_m}{E}(2N_f)^b+1.75\varepsilon_f'(2N_f)^c \tag{16}$$

$$\frac{\Delta\gamma_{max}}{2}=1.3\frac{\sigma_f'-\sigma_m}{E}(2N_f)^b+1.5\varepsilon_f'(2N_f)^c \tag{17}$$

where $\Delta\varepsilon_n$ is the strain range normal to the maximum shear strain plane, $\Delta\gamma_{max}$ is the maximum shear strain range, and σ_m is the mean stress.

Figure 10 and *Figure 11* represent the strain-life curves obtained from Brown-Miller [36] and maximum shear strain life [37] methods as well as the experimental data for specimens with notch root radii of 1.25, 2.5 and 5 mm at strain amplitude ranging from ± 0.4 to ± 0.8% at room temperature and 550°C respectively. As can be noticed, both criteria drastically underestimate the fatigue lives for all notch root size, all strain amplitude levels, and at both temperature loading conditions. The relative error is more significant at high-temperature than that at room temperature. The two criteria provide approximately the same relative error, with a slight increase in the relative error of 2.2 % on average when calculating the cyclic life based on the Brown-Miller approach [36]. For instance, in the case of a specimen with 2.5 mm notch radius,

subjected to ± 0.6% nominal strain amplitude, the relative errors using Brown-Miller [36] and maximum shear strain life [37] equations are -83.60 and -80.40 % respectively at room temperature, whereas at 550°C, the relative errors are -97.25 and -96.33% respectively. For the maximum shear strain life method [37], the relative error increases as the strain amplitude increase for all notch root size at higher temperature loading conditions. The same trend was observed at 550°C when using Brown-Miller method [36].

As it is noticed from *Table 4*, the fatigue lives obtained from both uniaxial and multiaxial low cycle fatigue life methods are inaccurate for all strain amplitude levels, all notch root radius and at both temperatures. This is due to the fact that the fatigue life is very sensitive to the calculated local strain, and any imprecise value of the notch strains will lead to an incorrect fatigue life estimation. Therefore, it is important to suggest a new method that allows the determination of the fatigue life using the nominal strain as an input parameter instead of the local strain.

4.3.3 Fatigue Life Estimation Based on the Proposed Method

In analogy with the elastic stress concentration factor [35], in the plastic range (i.e. plastic net section and plastic notch), one can assume that, under cyclic loading condition, the plastic stress concentration factor $K_{plastic}$ is the ratio of the plastic strain range at the notch root $\Delta\varepsilon_p$ to the plastic strain range developed in the net section Δe_p:

$$K_{plastic} = \frac{\Delta\varepsilon_p}{\Delta e_p} \tag{18}$$

According to Ramberg-Osgood [42], the local plastic strain range $\Delta\varepsilon_p$, and the nominal plastic strain range Δe_p can be expressed as follows:

$$\Delta\varepsilon_p = 2\left(\frac{\Delta\sigma}{2K'}\right)^{\frac{1}{n'}} \quad (19) \qquad \Delta e_p = 2\left(\frac{\Delta S}{2K'}\right)^{\frac{1}{n'}} \quad (20)$$

Substituting Eq. (19) and (20) in (18), one can obtain the following expression:

$$K_{plastic} = \left(\frac{\Delta\sigma}{\Delta S}\right)^{\frac{1}{n'}} \quad (21)$$

On the other hand, for Masing materials the plastic strain energy at the notch root ΔW_p and the plastic strain energy in the net section $\Delta W_p'$ are defined by the following equations [46].

$$\Delta W_p = \frac{1-n'}{1+n'}\Delta\sigma\Delta\varepsilon_p \quad (22) \qquad \Delta W_p' = \frac{1-n'}{1+n'}\Delta S\Delta e_p \quad (23)$$

Substituting Eq.(19) and (20) in (22) and (23) respectively, we get the following equations:

$$\Delta W_p = 2\left(\frac{1-n'}{1+n'}\right)\Delta\sigma\left(\frac{\Delta\sigma}{2K'}\right)^{\frac{1}{n'}} \quad (24) \qquad \Delta W_p' = 2\left(\frac{1-n'}{1+n'}\right)\Delta S\left(\frac{\Delta S}{2K'}\right)^{\frac{1}{n'}} \quad (25)$$

Rearranging Eq.(24) and (25), one can obtain:

$$\Delta\sigma = (2K')^{\frac{1}{n'+1}}\left(\frac{1+n'}{2(1-n')}\Delta W_p\right)^{\frac{n'}{1+n'}} \quad (26) \qquad \Delta S = (2K')^{\frac{1}{n'+1}}\left(\frac{1+n'}{2(1-n')}\Delta W_p'\right)^{\frac{n'}{1+n'}} \quad (27)$$

By substituting eq.(26) and (27) in (21) and rearranging, we get:

$$K_{plastic} = \left(\frac{\Delta W_p}{\Delta W_p'}\right)^{\frac{1}{1+n'}} \quad (28)$$

On the other hand, based on the Coffin-Manson [32,33] and Basquin [34] equations we have:

$$\Delta\sigma = 2\sigma_f'(2N_f)^b \quad (29) \qquad \Delta S = 2\sigma_f'(2N_f')^b \quad (30)$$

$$\Delta\varepsilon_p = 2\varepsilon_f'(2N_f)^c \quad (31) \qquad \Delta e_p = 2\varepsilon_f'(2N_f')^c \quad (32)$$

where N_f and N_f' are the fatigue life for notched and plain specimen respectively. Thus, by replacing Eq.(29) and (31) in (22), and Eq.(30) and (32) in (22) and (23) respectively ,one can obtain the following expressions:

$$\Delta W_p = 4\left(\frac{1-n'}{1+n'}\right)\sigma_f'\varepsilon_f'(2N_f)^{b+c} \qquad (33) \qquad \Delta W_p' = 4\left(\frac{1-n'}{1+n'}\right)\sigma_f'\varepsilon_f'(2N_f')^{b+c} \qquad (34)$$

Substituting Eq.(33) and (34) in (28) and rearranging, we obtain:

$$N_f{}^{b+c} = K_{plastic}^{1+n'} N_f'{}^{b+c} \qquad (35)$$

By determining the fatigue life of plain specimens using the Eq.(15), one can easily calculate the fatigue life of notched specimens using Eq.(35) under the same strain amplitude level. Where $K_{plastic}$ can be identified using the following Stowell's equation [47].

$$K_{plastic} = 1 + (K_t - 1)\frac{E_s}{E} \qquad (36)$$

where E_s is the secant modulus at a point of maximum stress, and it was determined using the following equation [47].

$$\frac{\sigma}{S} = 1 + 2\frac{E_s}{E} \qquad (37)$$

The obtained values of E_s from FEA are listed in *Table 5*, for each notch root size, strain amplitude level, and temperature loading. The calculated values of $K_{plastic}$ for 316LN stainless steel are also shown in the same table (i.e. *Table 5)*.

In the absence of the experimental fatigue data i.e. the fatigue strength exponent b and the fatigue strength exponent c, Morrow [48] suggested the two following approximations:

$$b \approx \frac{-n'}{1+5n'} \quad (38) \qquad c \approx \frac{-1'}{1+5n'} \quad (39)$$

And Eq. (35) becomes as follows:

$$N_f = K_{plastic}^{-(1+5n')} N_f' \quad (40)$$

By substituting Eq.(40) in (15) and rearranging, one can obtain the following expression:

$$\frac{\Delta\varepsilon_t}{2} = \frac{\Delta\varepsilon_e}{2} + \frac{\Delta\varepsilon_p}{2} = \frac{\sigma_f'}{E}\left(\frac{2N_f}{K_{plastic}^{-(1+5n')}}\right)^b + \varepsilon_f'\left(\frac{2N_f}{K_{plastic}^{-(1+5n')}}\right)^c \quad (41)$$

Thus, for a given nominal strain amplitude (i.e. $\Delta\varepsilon_t/2$), one can swiftly predict the fatigue life of a notched specimen using Eq.(41).

The calculated fatigue lives applying Eq. (35), along with the temperature dependent material parameters provided in Table 1, are represented in *Figure 12* and *Figure 13* for room temperature and 550°C, respectively. As evidenced, the suggested equation provides a better fatigue life prediction at elevated temperature and inadequate estimation at room temperature with an average relative error of -16.87 and 406.19%, respectively. The discrepancies between the estimated and the experimental results at ambient temperature are due to the fact that the 316LN SS exhibits a non-Masing behavior under this temperature loading condition, particularly at higher nominal strain amplitudes [25,49].Nerveless, this type of steel generally follows a Masing behavior at higher temperatures and nominal strain amplitudes level [49]. Moreover, as observed in *Table 4*, the suggested method provides a better fatigue life estimation at a high temperature compared to all the methods applied previously. For instance, for a specimen with 2.5 mm notch root radius, subjected to ± 0.6% nominal strain amplitude, the resulted relative error is only -8.72%. While the ones obtained from the uniaxial strain-life equation [32-34] using

the local strains found from Neuber's rule with $\mathrm{K_t}$ and $\mathrm{K_f}$ [1,5], ESED method [2,3], linear rule [35] and FEA are -94.50,-90.80, -89.45, -79.82 and -94.95 % respectively, and from the multiaxial strain-life equations Brown-Miller [36] and Maximum Shear strain methods are -97.25 and -96.33% respectively. It is worth to mention that the concept of non-Masing behavior is not addressed in this study, because, on the one hand, the equations of non-Masing analysis are complicated to be solved analytically, on the other hand, there is lack of experimental data in the literature to justify such a problem.

5 Conclusions

The local strains were estimated for cylindrical notched specimens made of 316 LN SS, with notch-root radius of 1.25, 2.5 and 5 mm, and subjected to strain amplitudes ranging from ± 0.4 to ± 0.8%, at room and elevated temperature by using various analytical approximations, this includes Neuber's rule with K_t [1], Neuber's rule with K_f [5], ESED method [2,3] and linear rule [35]. Based on the obtained local strains, the fatigue lives were predicted using the uniaxial strain-life equation [32-34] and the multiaxial low cycle fatigue equations [35,36]. The following conclusions can be made:

- A comparison of the local strains obtained from the better-known analytical approximations [1-3,5,35] with those found from FEA revealed that Neuber's rule with K_f [5], the ESED method [2,3], and the linear rule [35] underestimate the local strains, for all notch root radius, strain amplitude level and at both temperature loading conditions. However, Neuber's rule with K_t [1] overestimates the local strains at lower notch size,

namely at 1.25 mm under high temperature condition, while it underestimates the local strains at 2.5 mm and 5 mm at 550 °C, for all notch root radius at room temperature.

- The estimated fatigue lives based on the Manson-Coffin-Basquin equation [32-34], by using the numerically and analytically obtained local strains are inaccurate for all notch root radius, strain amplitudes and at both temperatures.
- The predicted fatigue lives from Brown-Miller [36] and Maximum Shear Strain [37] equations using Fe-safe software [43] showed that, in comparison to the experimental data, both multiaxial-low cycle fatigue criteria significantly underestimate the fatigue life results.
- The proposed method provides a better fatigue life prediction at higher temperature compared to all other methods for all notch root radius and under all applied strain amplitude. Nerveless, this method is not suitable for specimen made of 316LN SS loaded at higher nominal strain amplitudes, under room temperature loading condition, because this material exhibits a non-Masing behavior under this loading state.

ACKNOWLEDGMENT

The first author would like to acknowledge the CNRST (Centre National pour la Recherche Scientifique et Technique) in Rabat-Morocco for the Ph.D. grant.

NOMENCLATURE

FEA	Finite Element Analysis
ESED	Equivalent Strain Energy Density
SS	Stainless Steel
LCF	Low Cycle Fatigue
K_t	Elastic stress concentration factor
K_f	Fatigue stress concentration factor
$\Delta\sigma$	Local stress range
$\Delta\varepsilon$	Local strain range
K'	Cyclic strength coefficient
n'	Cyclic strain hardening exponent
E	Young's modulus
Δe	Nominal strain range
ΔS	Nominal stress range
q	Notch sensitivity factor
r	Notch root radius
ρ	Parameter depends on material properties
σ	Local stress
ε	Local strain
S	Nominal stress
e	Nominal strain
S_u	Ultimate tensile strength
$\Delta\varepsilon_e$	Elastic strain range
$\Delta\varepsilon_p$	Plastic strain range
σ_f'	Fatigue strength coefficient
ε_f'	Fatigue ductility coefficient
b	Fatigue strength exponent
c	Fatigue ductility exponent
N_f	Fatigue life of notched specimen

$\Delta\varepsilon_n$	Strain range normal to the maximum shear strain plane
$\Delta\gamma_{max}$	Maximum shear strain range
σ_m	Mean stress
$K_{plastic}$	Plastic stress concentration factor
Δe_p	Nominal plastic strain range
ΔW_p	Plastic strain energy at the notch root
$\Delta W_p'$	Plastic strain energy in the net section
N_f'	Fatigue life of plain specimen
E_s	Secant modulus at a point of maximum stress

REFERENCES

[1] Neuber, H., 1961, "Theory of stress concentration for shear-strained prismatical bodies with arbitrary nonlinear stress-strain law". Journal of Applied Mechanics 28(4), pp.544–50. doi.org/10.1115/1.3641780

[2] Molski, K. and Glinka, G., 1981, "A method of elastic-plastic stress and strain calculation at a notch root". Materials Science and Engineering, 50(1), pp.93-100. doi.org/10.1016/0025-5416(81)90089-6

[3] Glinka, G., 1985, "Energy density approach to calculation of inelastic strain-stress near notches and cracks". Engineering Fracture Mechanics, 22(3), pp.485-508. doi.org/10.1016/0013-7944(85)90148-1

[4] Ye, D., Hertel, O. and Vormwald, M., 2008," A unified expression of elastic–plastic notch stress–strain calculation in bodies subjected to multiaxial cyclic loading". International Journal of Solids and Structures, 45(24), pp.6177-6189. doi.org/10.1016/j.ijsolstr.2008.07.012

[5] Topper, T., Wetzel, R.M. and Morrow, J., 1967," Neuber's rule applied to fatigue of notched specimens". Illinois univ at Urbana dept of theoretical and applied mechanics.

[6] Hoffmann, M. and Seeger, T., 1985, "A generalized method for estimating multiaxial elastic-plastic notch stresses and strains", part 1: theory. doi.org/10.1115/1.3225814

[7] Seeger, T. and Heuler, P., 1980, "Generalized application of Neuber's rule". Journal of Testing and Evaluation, 8(4), pp.199-204. doi.org/10.1520/JTE11613J

[8] Stephens, R.I., Fatemi, A., Stephens, R.R. and Fuchs, H.O., 2000, "Metal fatigue in engineering". John Wiley & Sons.

[9] Wang, K.C. and Sharpe Jr, W.N., 1991," Evaluation of a modified cyclic Neuber relation". 113(3), pp.350–53. doi.org/10.1115/1.2903417

[10] Moftakhar, A., Buczynski, A. and Glinka, G., 1994, "Calculation of elasto-plastic strains and stresses in notches under multiaxial loading". International journal of fracture, 70(4), pp.357-373. doi.org/10.1007/BF00032453

[11] Singh, M.N.K., Glinka, G. and Dubey, R.N., 1996, "Elastic-plastic stress-strain calculation in notched bodies subjected to non-proportional loading". International journal of fracture, 76(1), pp.39-60. doi.org/10.1007/BF00034029

[12] Ye, D., Matsuoka, S., Suzuki, N. and Maeda, Y., 2004, "Further investigation of Neuber's rule and the equivalent strain energy density (ESED) method". International journal of fatigue, 26(5), pp.447-455. doi.org/10.1016/j.ijfatigue.2003.10.002

[13] Campagnolo, A., Berto, F. and Marangon, C., 2016, "Cyclic plasticity in three-dimensional notched components under in-phase multiaxial loading at R=− 1". Theoretical and Applied Fracture Mechanics, 81, pp.76-88. doi.org/10.1016/j.tafmec.2015.10.004

[14] Li, J., Zhang, Z.P. and Li, C.W., 2017, "Elastic-plastic stress-strain calculation at notch root under monotonic, uniaxial and multiaxial loadings". Theoretical and Applied Fracture Mechanics, 92, pp.33-46. doi.org/10.1016/j.tafmec.2017.05.005

[15] Zhu, S.P., Xu, S., Hao, M.F., Liao, D. and Wang, Q., 2019, "Stress-strain calculation and fatigue life assessment of V-shaped notches of turbine disk alloys". Engineering Failure Analysis, 106, pp.104187. doi.org/10.1016/j.engfailanal.2019.104187

[16] Barkey, M.E., Socie, D.F. and Hsia, K.J., 1994, "A yield surface approach to the estimation of notch strains for proportional and non-proportional cyclic loading" Journal of Engineering Materials and Technology 116 (2), pp.173–80. doi.org/10.1115/1.2904269

[17] Köttgen, V.B., Barkey, M.E. and Socie, D.F., 1995, "Pseudo stress and pseudo strain based approaches to multiaxial notch analysis". Fatigue & fracture of engineering materials & structures, 18(9), pp.981-1006. doi.org/10.1111/j.1460-2695.1995.tb00922.x

[18] Hertel, O., Vormwald, M., Seeger, T., Döring, R. and Hoffmeyer, J., 2005,"Notch stress and strain approximation procedures for application with multiaxial nonproportional loading": This contribution represents an extended version of a keynote given during the 7th International Conference on Biaxial/Multiaxial Fatigue and Fracture (7th ICBMFF). Materials Testing, 47(5), pp.268-277. doi.org/10.3139/120.100656

[19] Jiang, Y. and Sehitoglu, H., 1996, “Modeling of cyclic ratchetting plasticity, part I: development of constitutive relations”. Journal of Applied Mechanics, 63(3), pp.720–25. doi.org/10.1115/1.2823355

[20] Firat, M., 2011, “A notch strain calculation of a notched specimen under axial-torsion loadings”. Materials & Design, 32(7), pp.3876-3882. doi.org/10.1016/j.matdes.2011.03.005

[21] Chaboche, J.L., 1989, “Constitutive equations for cyclic plasticity and cyclic viscoplasticity”. International journal of plasticity, 5(3), pp.247-302. doi.org/10.1016/0749-6419(89)90015-6

[22] Antoni, N., 2019, “A novel rapid method of purely elastic solution correction to estimate multiaxial elastic-plastic behaviour”. Journal of Computational Design and Engineering, 6(3), pp.269-283. doi.org/10.1016/j.jcde.2019.01.002

[23] Prasad, Y.V.R.K., Rao, K.P. and Sasidhar, S. eds., 2015, “Hot working guide: a compendium of processing maps”. ASM international.

[24] Basu, K., Das, M., Bhattacharjee, D. and Chakraborti, P.C., 2007, “Effect of grain size on austenite stability and room temperature low cycle fatigue behaviour of solution annealed AISI 316LN austenitic stainless steel”. Materials Science and Technology, 23(11), pp.1278-1284. doi.org/10.1179/174328407X179575

[25] Roy, S.C., Goyal, S., Sandhya, R. and Ray, S.K., 2012, “Low cycle fatigue life prediction of 316 L (N) stainless steel based on cyclic elasto-plastic response”. Nuclear engineering and design, 253, pp.219-225. doi.org/10.1016/j.nucengdes.2012.08.024

[26] Wu, H.C., Yang, B., Wang, S.L. and Zhang, M.X., 2015,” Effect of oxidation behavior on the corrosion fatigue crack initiation and propagation of 316LN austenitic stainless steel in high temperature water”. Materials Science and Engineering: A, 633, pp.176-183. doi.org/10.1016/j.msea.2015.03.026

[27] Yuan, X., Yu, W., Fu, S., Yu, D. and Chen, X., 2016,” Effect of mean stress and ratcheting strain on the low cycle fatigue behavior of a wrought 316LN stainless steel”. Materials Science and Engineering: A, 677, pp.193-202. doi.org/10.1016/j.msea.2016.09.053

[28] Xiong, Y., Watanabe, Y. and Shibayama, Y., 2020, “Effects of dissolved hydrogen on low-cycle fatigue behaviors and hydrogen uptake of 316LN austenitic stainless steel in simulated pressurized water reactor primary water”. International Journal of Fatigue, 134, pp.105457. doi.org/10.1016/j.ijfatigue.2019.105457

[29] Abarkan, I., Shamass, R., Achegaf, Z. and Khamlichi, A., 2020, “Numerical and analytical studies of low cycle fatigue behavior of 316 LN austenitic stainless steel”. Journal of Pressure Vessel Technology. doi.org/10.1115/1.4045897

[30] Goyal, S., Veerababu, J., Sandhya, R., Laha, Knd Bhaduri, A.K., 2016, “Effect of notch on low cycle fatigue behaviour of 316 LN stainless steel”. Transactions of the Indian Institute of Metals, 69(5), pp.1015-1022. doi.org/10.1007/s12666-015-0609-6

[31] Agrawal, R., Veerababu, J., Goyal, S., Sandhya, R., Uddanwadiker, R. and Padole, P., 2018, “Estimation of Low Cycle Fatigue Response of 316 LN Stainless Steel in the Presence of Notch”. Journal of Materials Engineering and Performance, 27(2), pp.590-600. doi.org/10.1007/s11665-018-3149-5

[32] Coffin Jr, L.F., 1954,” A study of the effects of cyclic thermal stresses on a ductile metal”. Transactions of the American Society of Mechanical Engineers, New York, 76, pp.931-950.

[33] Manson, S.S., 1953, "Behavior of materials under conditions of thermal stress ". Washington, D.C.: National Advisory Committee for Aeronautics.

[34] Basquin, O.H., 1910, “The exponential law of endurance tests”. In Proc Am Soc Test Mater (Vol. 10, pp. 625-630).

[35] Gowhari-Anaraki, A.R. and Hardy, S.J., 1991,” Low cycle fatigue life predictions for hollow tubes with axially loaded axisymmetric internal projections”. The Journal of Strain Analysis for Engineering Design, 26(2), pp.133-146. doi.org/10.1243/03093247V262133

[36] Brown, M.W. and Miller, K.J., 1973,” A theory for fatigue failure under multiaxial stress-strain conditions”. Proceedings of the Institution of Mechanical engineers, 187(1), pp.745-755. doi.org/10.1243/PIME_PROC_1973_187_161_02

[37] Fatemi, A. and Shamsaei, 2011,” N. Multiaxial fatigue: An overview and some approximation models for life estimation”. Int. J. Fatigue, 33(8), pp. 948–958. doi.org/10.1016/j.ijfatigue.2011.01.003

[38] Morrow, J., 1968,” Fatigue design handbook”. Advances in engineering, 4, pp.21-29.

[39] Abaqus 6.11, 2011, Dassault Systemes Simulia Corp Providence, RI, USA

[40] Veerababu, J., Goyal, S., Sandhya, R. and Laha, K., 2017,” Fatigue life estimation of notched specimens of modified 9Cr-1Mo steel under uniaxial cyclic loading”. Materials at High Temperatures, 34(4), pp.250-259. doi.org/10.1080/09603409.2017.1308084

[41]Chaboche,J.L.,1986,”Time-independent constitutive theories for cyclic plasticity”. International Journal of plasticity, 2(2), pp.149-188. doi.org/10.1016/0749-6419 (86)90010-0

[42] Klesnil, M., & Lukác, P. 1980, “Fatigue of metallic materials”. Amsterdam: Elsevier. vol. 71.

[43] Peterson RE., 1974, “Stress concentration factors”. New York(NY): Wiley.

[44] Fe-Safe 6.2, 2011, Dassault Systemes Simulia, Corp Providence RI, USA

[45] Dassault Systemes Simulia Corp., 2014,”Fatigue Theory Reference Manual”. Safe Technology Limited. vol. 2.

[46] Golos, K. and Ellyin, F., 1989,”Total strain energy density as a fatigue damage parameter”. In Advances in Fatigue Science and Technology (pp. 849-858). Springer, Dordrecht. doi.org/10.1007/978-94-009-2277-8_42

[47] Stowell, E.Z., 1950,” Stress and strain concentration at a circular hole in an infinite plate”. Washington, D.C.: National Advisory Committee for Aeronautics.

[48] Morrow, J., 1965,” Cyclic plastic strain energy and fatigue of metals. In Internal friction, damping, and cyclic plasticity”. ASTM International. doi.org/10.1520/STP43764S

[49] Goyal, S., Mandal, S., Parameswaran, P., Sandhya, R., Athreya, C.N. and Laha, K., 2017,” A comparative assessment of fatigue deformation behavior of 316 LN SS at ambient and high temperature”. Materials Science and Engineering: A, 696, pp.407-415. doi.org/10.1016/j.msea.2017.04.102

Table Caption List

Table 1 Static and cyclic properties of 316LN SS at room temperature, and 550 °C [31].

Table 2 The obtained values of K_t , and K_f at different notch root radii for 316LN SS.

Table 3 Relative error values between the analytical and numerical obtained local strains under each applied strain amplitude for notch root radii of 1.25, 2.5, and 5 mm, at room temperature and 550 °C.

Table 4 Relative error values between the experimental and predicted fatigue life for different imposed strain amplitudes and for notch root radii of 1.25, 2.5, and 5 mm, at room temperature and 550 °C.

Table 5 The secant modulus and plastic stress concentration factor of 316LN SS at a point of maximum stress for each notch root radius at different stain amplitudes at room temperature, and 550 °C.

Figure Captions List

Fig. 1 Shape and dimensions of smooth specimens (all dimensions are in mm).

Fig. 2 Shape and dimensions of (a) notched specimens, with different notch root radius, (b) 1.25 mm, (c) 2.5 mm, and (d) 5 mm, (all dimensions are in mm).

Fig. 3 Finite element modeling of a 2D-axisymmetric part with 2.5 mm notch root size, (a) mesh refinement, and (b) boundary conditions and loading.

Fig. 4 A comparison between the experimental hysteresis loops found by Veerababu et al. [40], and the ones obtained from FEA for a plain specimen made of 9Cr-1Mo steel, under (a) ± 0.3 %, and (b) ±0.8 % strain amplitudes, at 550 °C temperature loading.

Fig. 5 A comparison between the first hysteresis loop at the notch-root, obtained from the current FE simulation and the one resulted from Veerababu et al. [40] FEA, for a notched specimen with 2.5 mm notch root radius, under ±149.95 MPa nominal stress amplitude, at 550 °C temperature loading.

Fig. 6 Comparison between the elastic-plastic strains obtained from FEA and the analytical methods for different strain amplitudes at room temperature for (a) 1.25 mm, (b) 2.5 mm, and (c) 5 mm notch root radii.

Fig. 7 Comparison between the elastic-plastic strains obtained from FEA and the analytical methods for different strain amplitudes at 550 °C for (a) 1.25 mm, (b) 2.5 mm, and (c) 5 mm notch root radii.

Fig. 8 Comparison between the experimental and estimated fatigue life from the uniaxial fatigue life method for different strain amplitudes at room temperature for (a) 1.25 mm, (b) 2.5 mm, and (c) 5 mm notch root radii.

Fig. 9 Comparison between the experimental and estimated fatigue life from the uniaxial fatigue life method for different strain amplitudes at 550 °C for (a) 1.25 mm, (b) 2.5 mm, and (c) 5 mm notch root radii.

Fig. 10 Comparison between the experimental fatigue life and the fatigue life obtained from Brown-Miller and Maximum shear strain methods for different strain amplitudes at room temperature for (a) 1.25 mm, (b) 2.5 mm, and (c) 5 mm notch root radii.

Fig. 11 Comparison between the experimental fatigue life and the fatigue life obtained from Brown-Miller and Maximum shear strain methods for different strain amplitudes at 550 °C for (a) 1.25 mm, (b) 2.5 mm, and (c) 5 mm notch root radii.

Fig. 12 Comparison between the experimental fatigue life and the fatigue life obtained from the proposed method for different strain amplitudes at room temperature for (a) 1.25 mm, (b) 2.5 mm, and (c) 5 mm notch root radii.

Fig. 13 Comparison between the experimental fatigue life and the fatigue life obtained from the proposed method for different strain amplitudes at 550 °C for (a) 1.25 mm, (b) 2.5 mm, and (c) 5 mm notch root radii.

Table 1: *Static and cyclic properties of 316LN SS at room temperature, and* 550 °C [31].

Temperature	Young's modulus E (GPa)	Yield strength S_y (MPa)	Cyclic strength coefficient K'(MPa)	Cyclic strain hardening exponent n'	Fatigue strength coefficient σ_f' (MPa)	Fatigue strength exponent b	Fatigue ductility coefficient ε_f'	fatigue ductility exponent c
Room Temperature	200	268	1393	0.275	2636	-0.22	0.6501	-0.541
550 ℃	155	117	2267	0.354	1359	-0.161	0.08453	-0.394

Table 2: *The obtained values of K_t , and K_f at different notch root radii for 316LN SS.*

r (mm)	K_t	K_f
1.25	3.91	3.31
2.5	3.13	2.89
5	2.62	2.52

Table 3: *Relative error values between the analytical and numerical obtained local strains under each applied strain amplitude for notch root radii of 1.25, 2.5, and 5 mm, at room temperature and 550 °C.*

Temperature	Notch root radius (mm)	Nominal Strain amplitude %	Relative error % $= \left(\frac{\Delta\varepsilon^{Analytical}}{\Delta\varepsilon^{Numerical}} - 1\right) \times 100\%$			
			Neuber K_t	Neuber K_f	ESED	Linear rule
Room temperature	1.25	0.4	-9.69	-23.90	-29.55	-55.35
		0.6	-10.00	-24.21	-35.10	-56.35
		0.8	-10.59	-24.74	-35.84	-57.08
	2.5	0.4	-23.55	-29.49	-43.85	-57.30
		0.6	-25.08	-30.93	-45.59	-58.93
		0.8	-24.76	-30.64	-45.70	-59.10
	5	0.4	-40.52	-39.02	-53.17	-61.20
		0.6	-38.00	-45.16	-54.65	-62.54
		0.8	-39.93	-41.99	-56.36	-63.99
550 °C	1.25	0.4	8.83	-14.36	-14.49	-36.99
		0.6	7.98	-15.13	-15.74	-38.99
		0.8	7.50	-15.59	-16.91	-40.10
	2.5	0.4	-1.68	-12.32	-21.99	-37.30
		0.6	-3.61	-20.35	-24.45	-39.87
		0.8	-5.92	-16.17	-26.80	-42.10
	5	0.4	-14.43	-19.07	-31.48	-41.13
		0.6	-15.81	-29.17	-33.53	-43.23
		0.8	-18.65	-23.09	-36.31	-45.76

Table 4: *Relative error values between the experimental and predicted fatigue life for different imposed strain amplitudes and for notch root radii of 1.25, 2.5, and 5 mm, at room temperature and 550 °C.*

Temperature	Notch root radius (mm)	Nominal Strain amplitude %	Relative error % $= \left(\frac{{N_f}^{Predicted}}{{N_f}^{Test}} - 1\right) \times 100\%$							
			Neuber K_t	Neuber K_f	Linear rule	ESED	FEA	Brown-Miller	Maximum shear strain	Suggested equation
Room temperature	1.25	0.4	-52.41	-33.14	96.88	-22.10	-61.19	-72.80	-68.56	506.80
		0.6	-56.55	-39.29	81.55	-17.86	-64.88	-77.38	-72.02	452.38
		0.8	-64.35	-50.43	48.70	-32.17	-71.30	-81.74	-79.13	333.91
	2.5	0.4	-44.96	-35.04	82.31	3.14	-67.77	-76.86	-72.73	465.12
		0.6	-49.10	-40.20	70.11	-3.56	-71.17	-83.60	-80.40	421.35
		0.8	-41.61	-31.39	94.89	10.20	-66.42	-77.37	-72.99	478.10
	5	0.4	-48.71	-51.29	24.86	-15.90	-82.07	-86.44	-83.48	272.02
		0.6	-43.38	-27.63	57.08	6.16	-78.08	-82.42	-80.37	357.53
		0.8	-40.52	-36.64	65.09	12.10	-78.02	-82.76	-80.60	368.53
550 °C	1.25	0.4	-93.48	-86.52	-67.39	-86.52	-91.30	-94.78	-93.91	-27.83
		0.6	-94.95	-90.91	-76.77	-89.90	-93.94	-96.97	-96.97	-7.07
		0.8	-95.45	-90.91	-77.27	-88.64	-93.18	-97.73	-95.45	-15.91
	2.5	0.4	-94.61	-92.53	-79.67	-89.49	-94.88	-96.68	-96.13	-49.38
		0.6	-94.50	-90.80	-79.82	-89.45	-94.95	-97.25	-96.33	-8.72
		0.8	-94.90	-92.86	-80.61	-89.80	-95.92	-97.96	-96.94	-18.37
	5	0.4	-88.92	-86.87	-65.25	-78.25	-93.02	-95.08	-93.71	-12.86
		0.6	-92.97	-88.38	-77.37	-85.93	-95.72	-96.94	-96.02	6.12
		0.8	-94.05	-92.86	-80.90	-88.10	-96.43	-97.62	-97.02	-17.86

Table 5: *The secant modulus and plastic stress concentration factor of 316LN SS at a point of maximum stress for each notch root radius at different stain amplitudes at room temperature, and 550 ℃.*

Temperature	Nominal Strain amplitude %	**1.25 mm**		**2.5 mm**		**5 mm**	
		$E_s(MPa)$	$K_{plastic}$	$E_s(MPa)$	$K_{plastic}$	$E_s(MPa)$	$K_{plastic}$
Room temperature	0.4	136547	3.00	119275	2.27	106259	1.86
	0.6	127055	2.85	109997	2.17	98688	1.80
	0.8	125931	2.83	108086	2.15	96680	1.78
550°C	0.4	117962	3.21	97263	2.32	81330	1.85
	0.6	115061	3.16	94805	2.30	79624	1.83
	0.8	113228	3.13	93471	2.28	78592	1.82

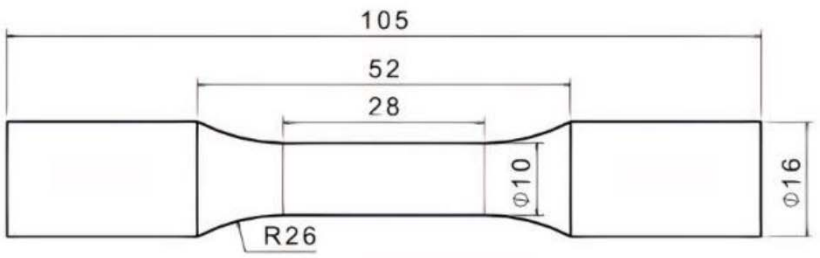

***Fig. 1**:* Shape and dimensions of smooth specimens (all dimensions are in mm).

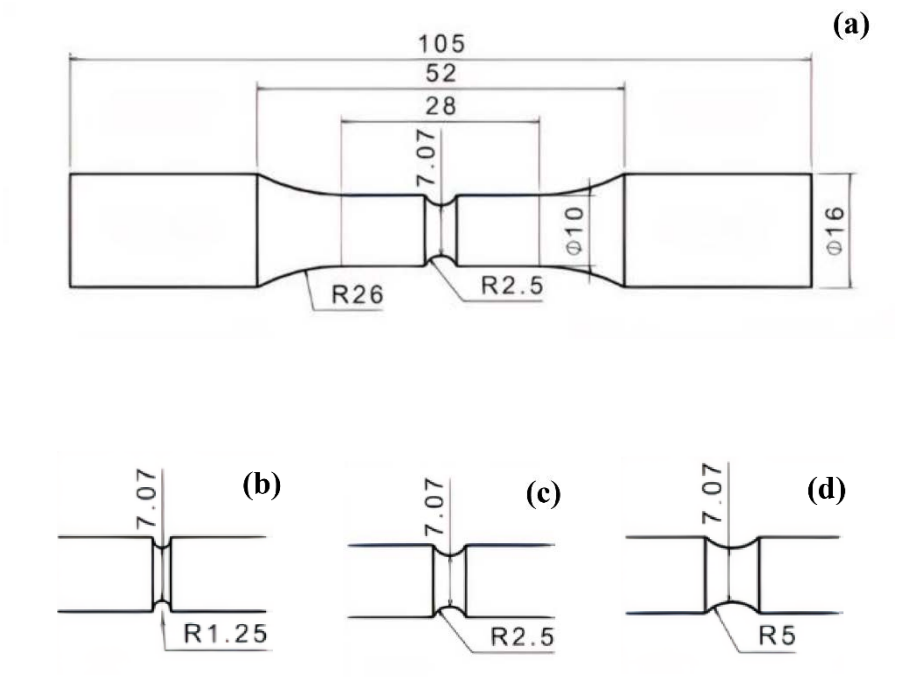

Fig. 2*:* Shape and dimensions of (a) notched specimens, with different notch root radius, (b) 1.25 mm, (c) 2.5 mm, and (d) 5 mm, (all dimensions are in mm).

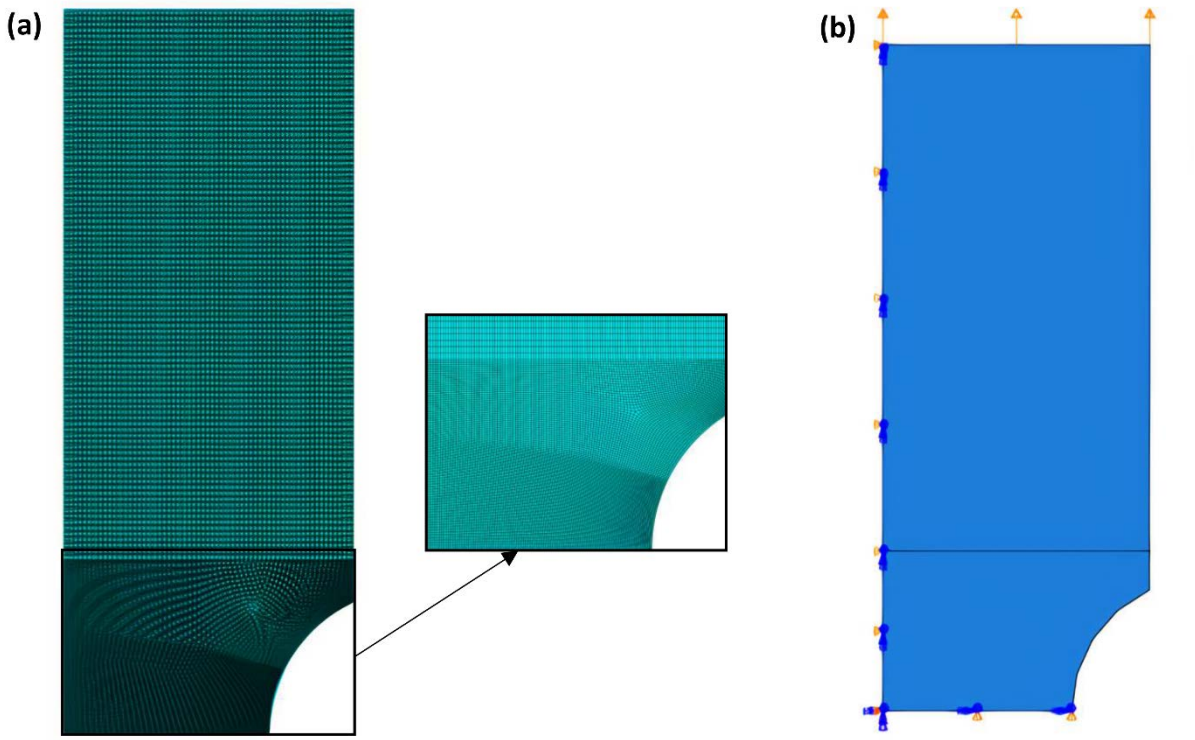

Fig. 3*: Finite element modeling of a 2D-axisymmetric part with 2.5 mm notch root size, (a) mesh refinement, and (b) boundary conditions and loading.*

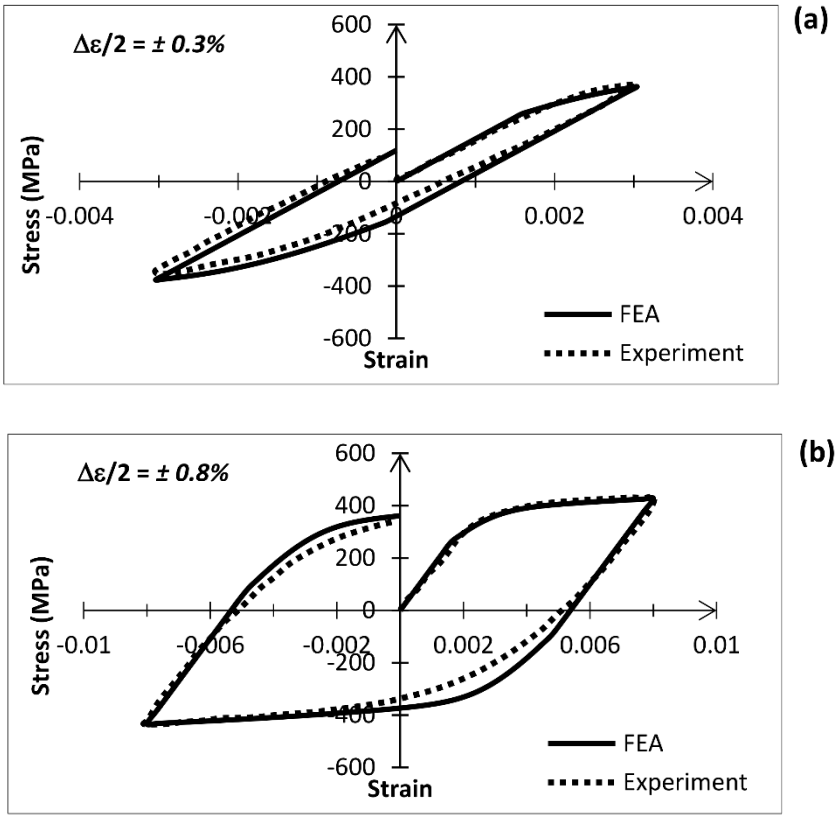

Fig. 4*: A comparison between the experimental hysteresis loops found by Veerababu et al. [40], and the ones obtained from FEA for a plain specimen made of 9Cr-1Mo steel, under (a) ± 0.3 %, and (b) ± 0.8 % strain amplitudes, at 550 °C temperature loading.*

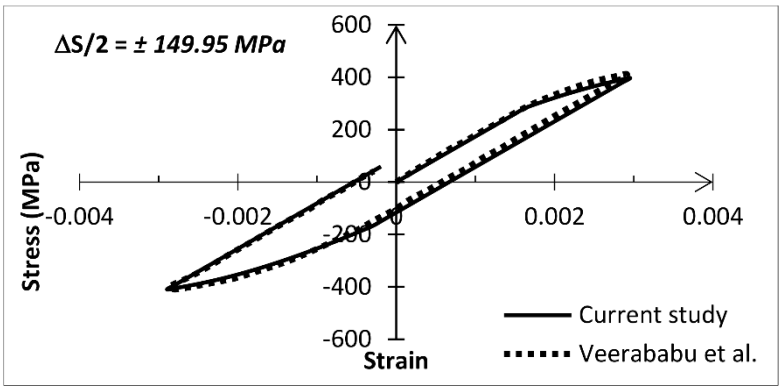

Fig. 5*: A comparison between the first hysteresis loop at the notch-root, obtained from the current FE simulation and the one resulted from Veerababu et al. [40] FEA, for a notched specimen with 2.5 mm notch root radius, under ± 149.95 MPa nominal stress amplitude, at 550 °C temperature loading.*

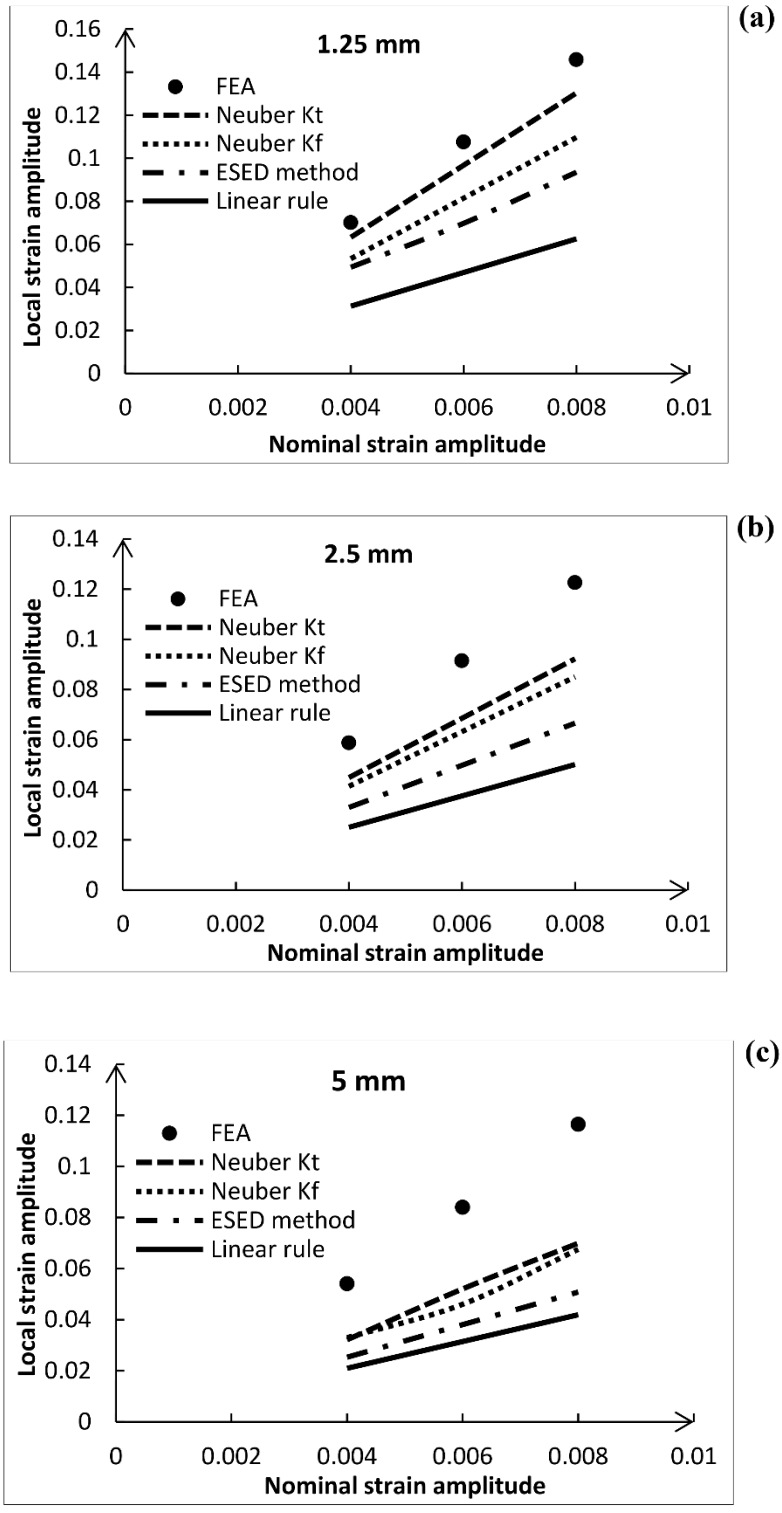

Fig. 6: *Comparison between the elastic-plastic strains obtained from FEA and the analytical methods for different strain amplitudes at room temperature for (a) 1.25 mm, (b) 2.5 mm, and (c) 5 mm notch root radii.*

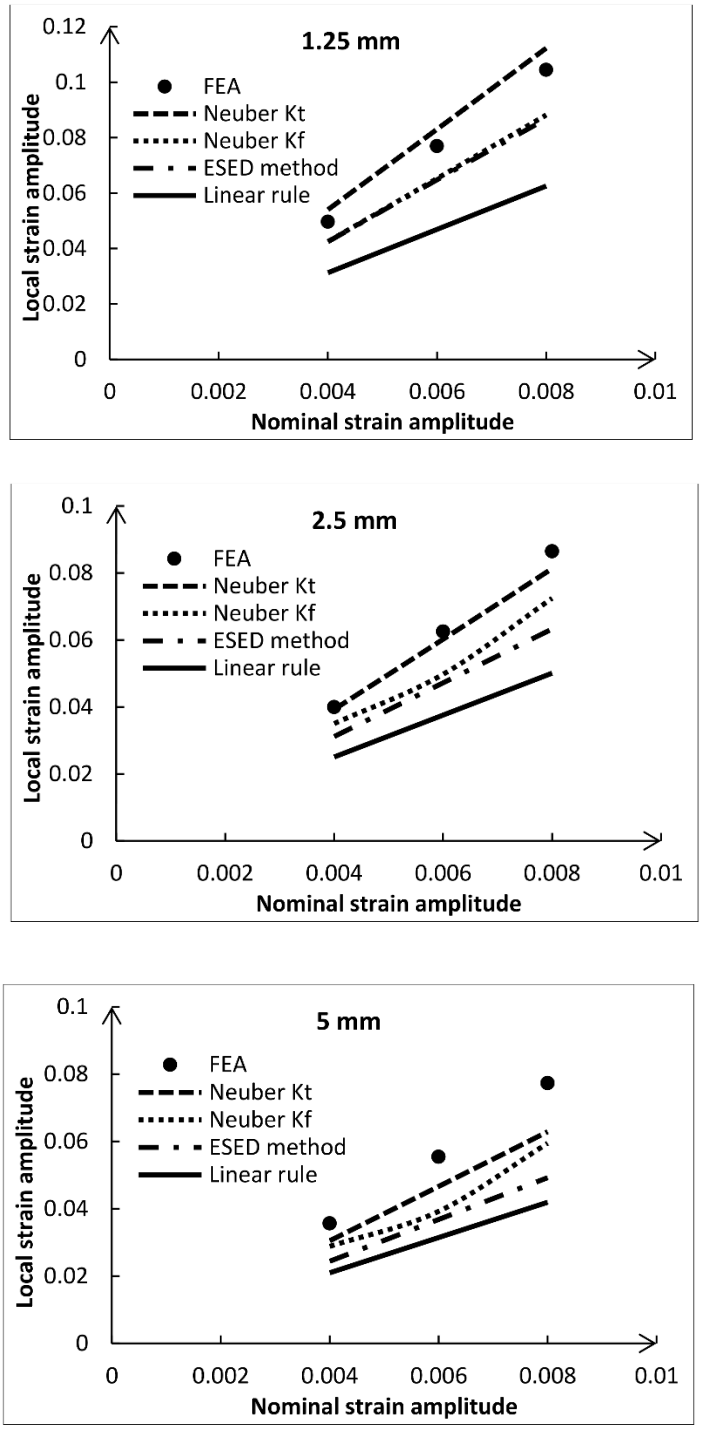

Fig. 7: *Comparison between the elastic-plastic strains obtained from FEA and the analytical methods for different strain amplitudes at 550 °C for (a) 1.25 mm, (b) 2.5 mm, and (c) 5 mm notch root radii.*

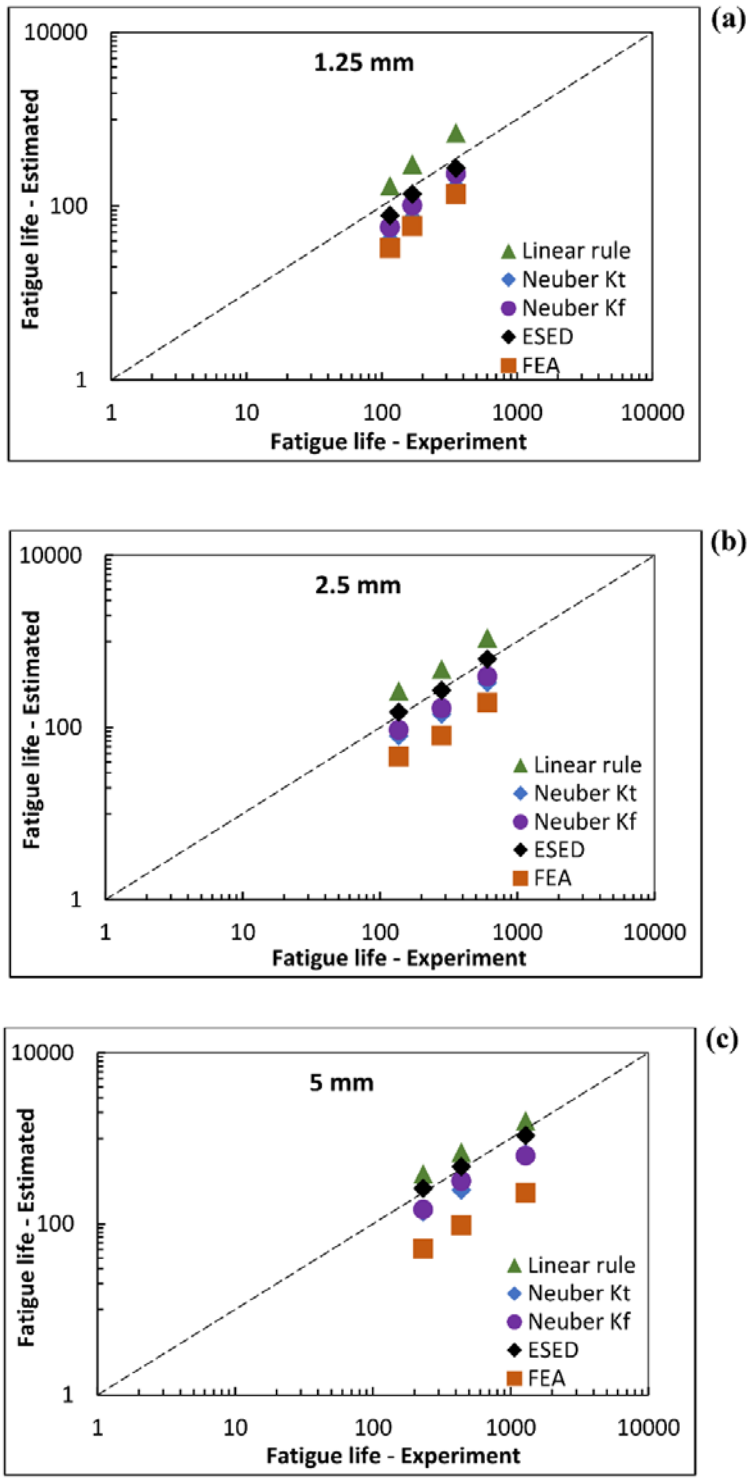

Fig. 8: *Comparison between the experimental and estimated fatigue life from the uniaxial fatigue life method for different strain amplitudes at room temperature for (a) 1.25 mm, (b) 2.5 mm, and (c) 5 mm notch root radii.*

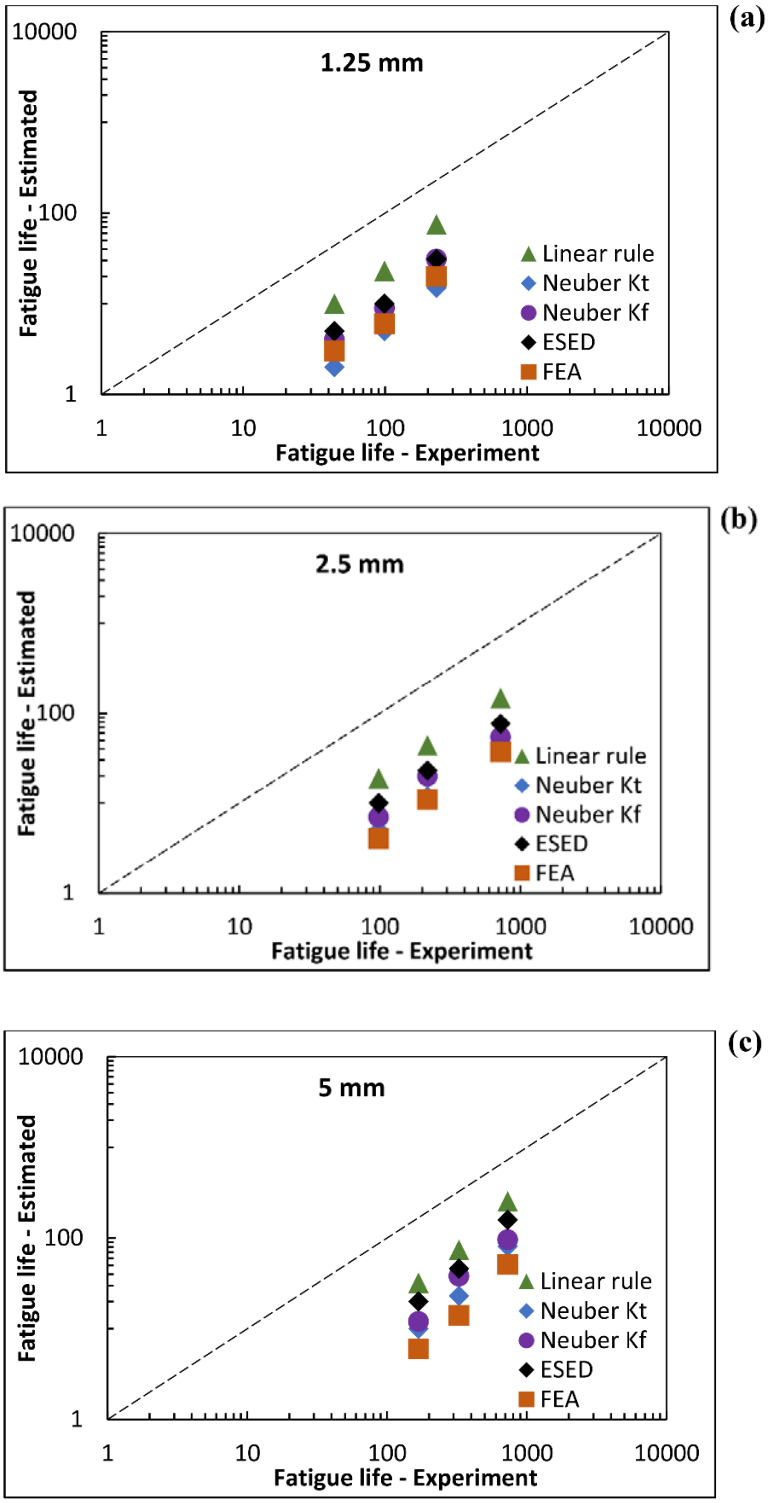

Fig. 9: *Comparison between the experimental and estimated fatigue life from the uniaxial fatigue life method for different strain amplitudes at 550 °C for (a) 1.25 mm, (b) 2.5 mm, and (c) 5 mm notch root radii.*

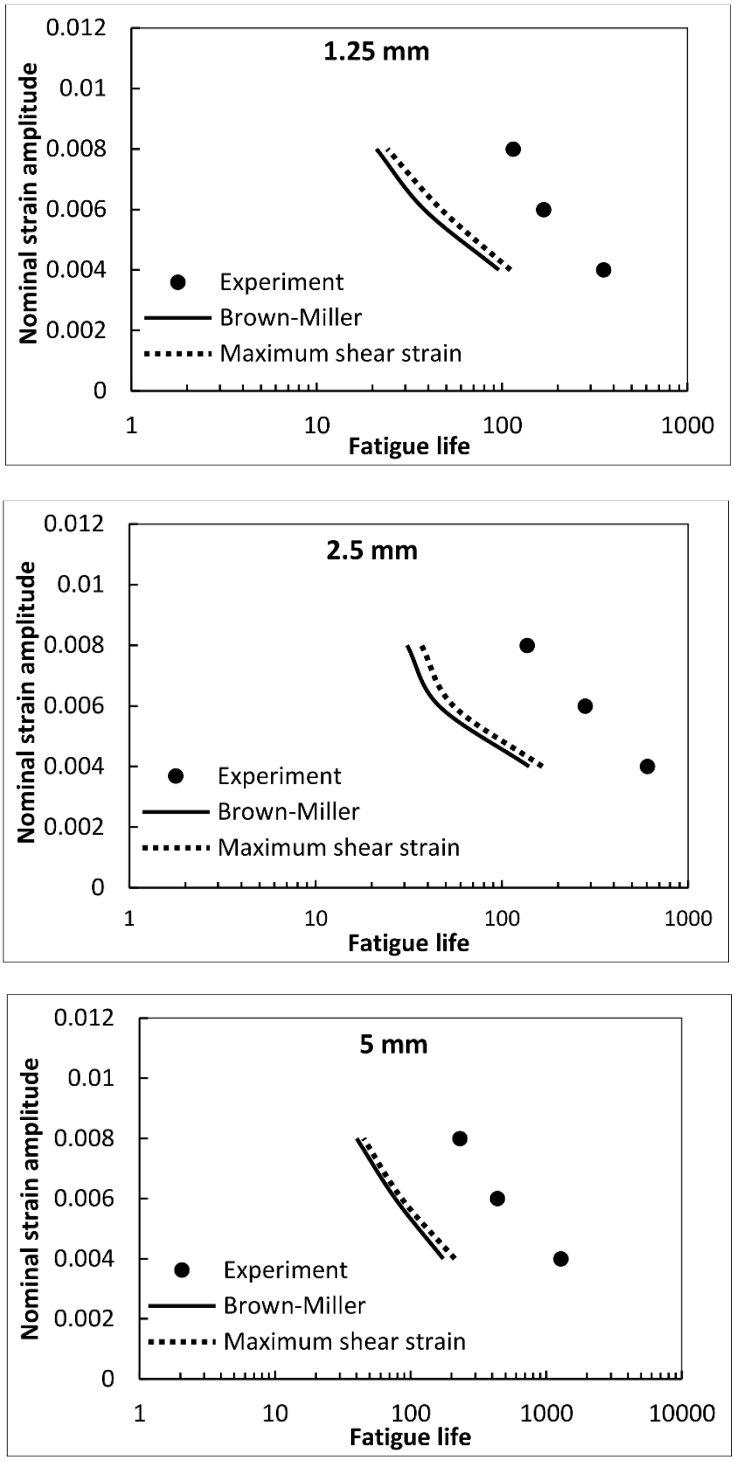

Fig. 10: *Comparison between the experimental fatigue life and the fatigue life obtained from Brown-Miller and Maximum shear strain methods for different strain amplitudes at room temperature for (a) 1.25 mm, (b) 2.5 mm, and (c) 5 mm notch root radii.*

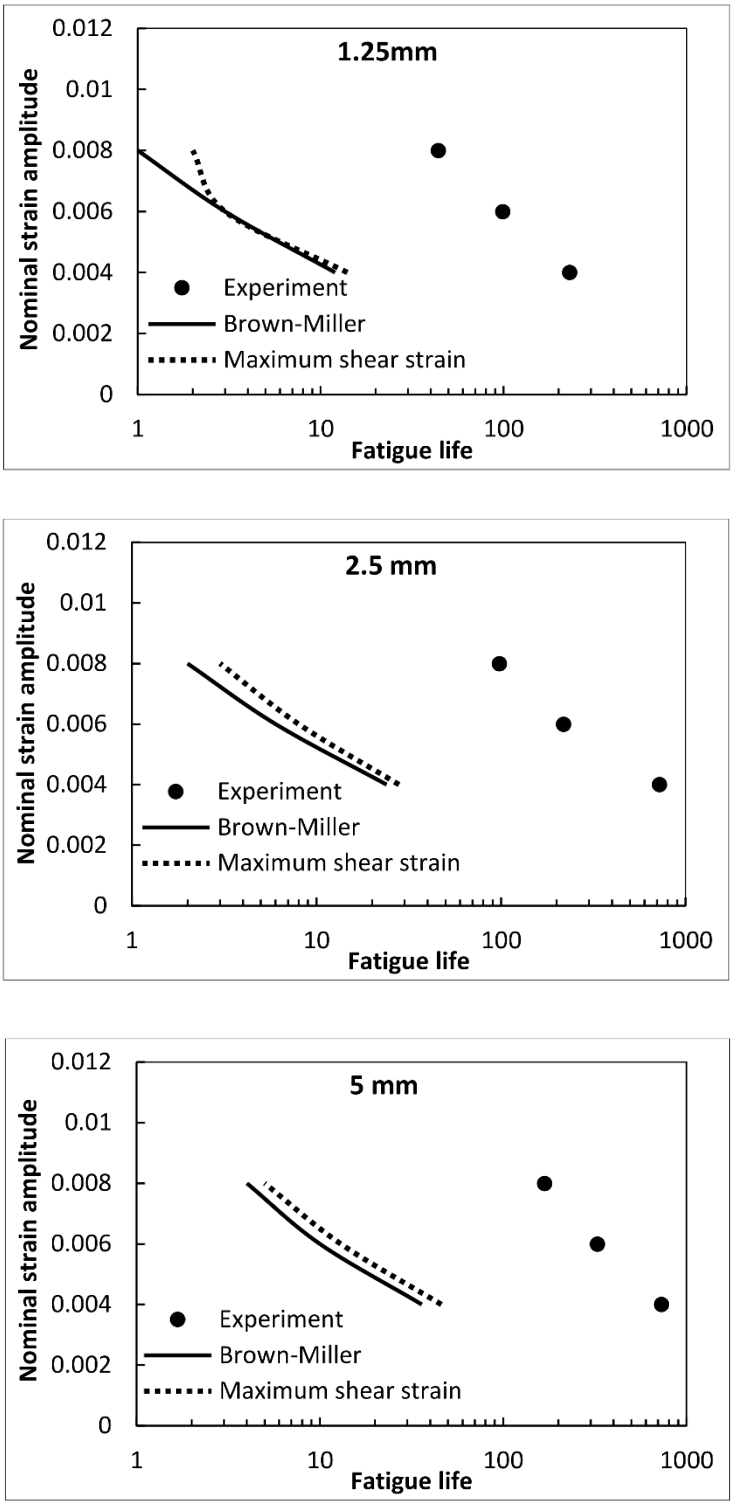

Fig. 11: *Comparison between the experimental fatigue life and the fatigue life obtained from Brown-Miller and Maximum shear strain methods for different stain amplitudes at 550 °C for (a) 1.25 mm, (b) 2.5 mm, and (c) 5 mm notch root radii.*

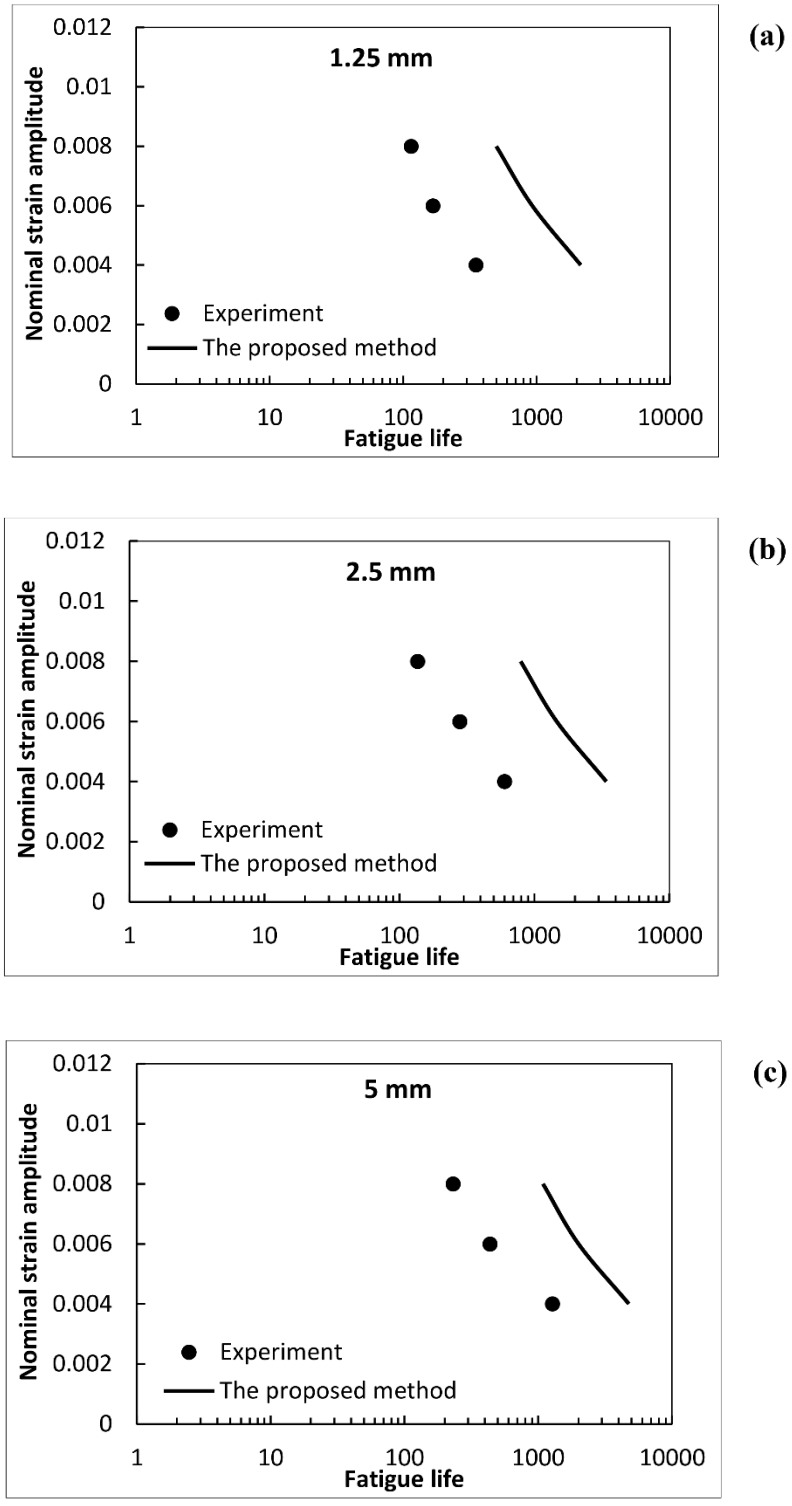

Fig.12: *Comparison between the experimental fatigue life and the fatigue life obtained from the proposed method for different strain amplitudes at room temperature for (a) 1.25 mm, (b) 2.5 mm, and (c) 5 mm notch root radii.*

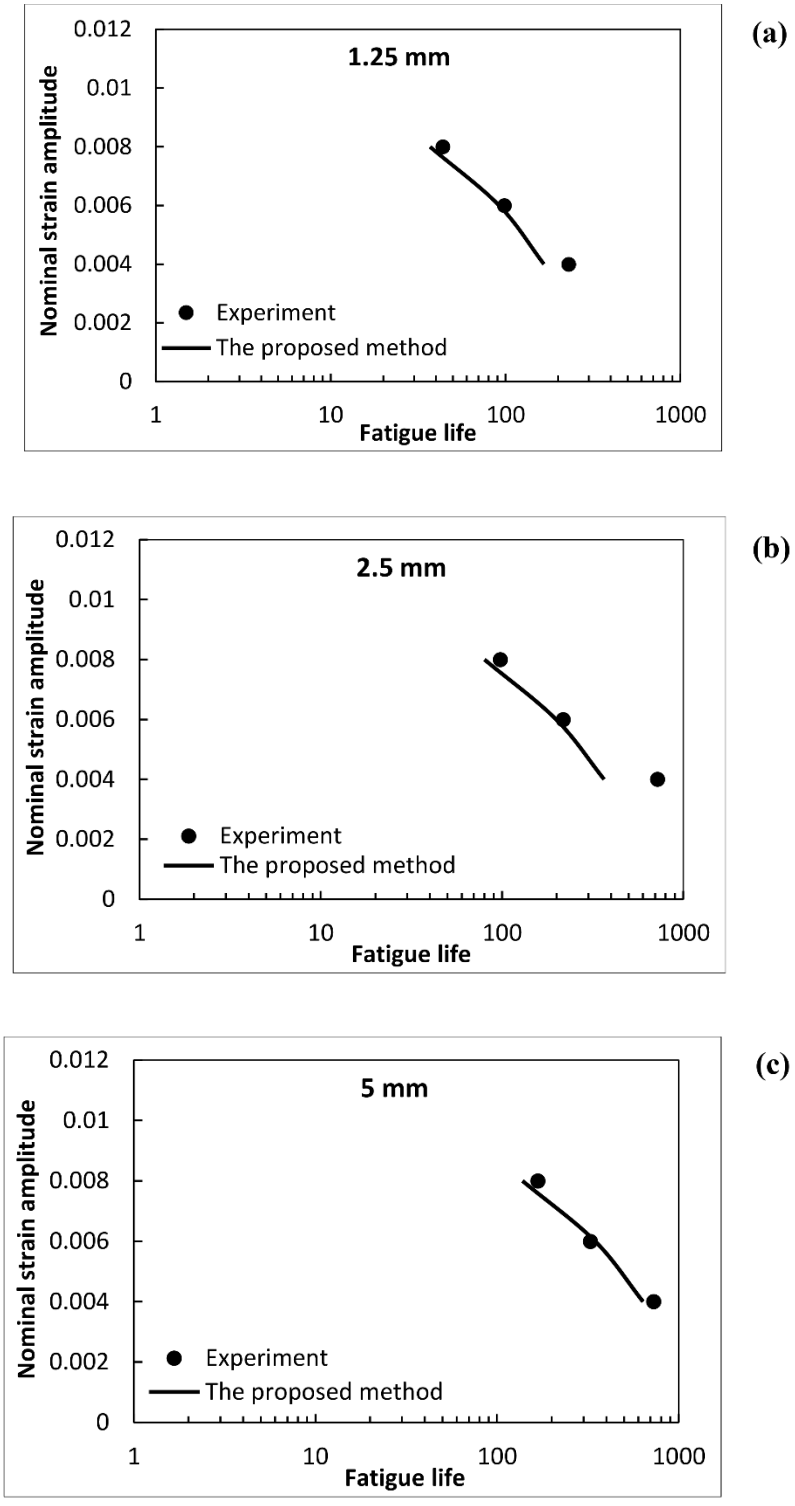

Fig. 13: *Comparison between the experimental fatigue life and the fatigue life obtained from the proposed method for different strain amplitudes at 550 °C for (a) 1.25 mm, (b) 2.5 mm, and (c) 5 mm notch root radii.*